Taylor & Francis
Taylor & Francis Group

Check for updates

Synthesis, spectral characterization, DNA-binding and antimicrobial profile of biological active mixed ligand Schiff base metal(II) complexes incorporating 1,8-diaminonaphthalene

Thiravidamani Chandrasekar, Alagarraj Arunadevi and Natarajan Raman

Research Department of Chemistry, VHNSN College, Virudhunagar, Tamil Nadu, India

ABSTRACT

Mixed-ligand complexes of bivalent metal ions, *viz*, Co(II), Ni(II), Cu(II), and Zn(II) of the composition [ML(dan)]Cl (where L = Schiff base ligand, dan = 1,8-diaminonaphthalene and M = Co(II), Ni(II), Cu(II), Zn(II)) have been synthesized and characterized. The stoichiometric ratio of the prepared complexes has been estimated using complementary techniques such as elemental analyses, FT-IR, UV-vis and EPR spectra, magnetic and molar conductivity measurements. The study shows that all the complexes have square planar geometry. The synthesized compounds have been tested *in vitro* against various types of pathogenic bacteria to weigh up their antimicrobial properties. They have lofty activity against the tested bacteria. The complexes have higher activity than the free ligands. The interaction of synthesized complexes with calf thymus DNA (CT-DNA) has been studied by absorption spectroscopic technique and viscosity measurements. The complexes show a successful interaction with CT-DNA *via* intercalation mode. In addition, molecular docking approach has been performed for predicting the binding free energy of the synthesized compounds with 1BNA receptor.

CONTACT Natarajan Raman ✉ ramchem1964@gmail.com 🖃 Research Department of Chemistry, VHNSN College, Virudhunagar 626 001, Tamil Nadu, India.
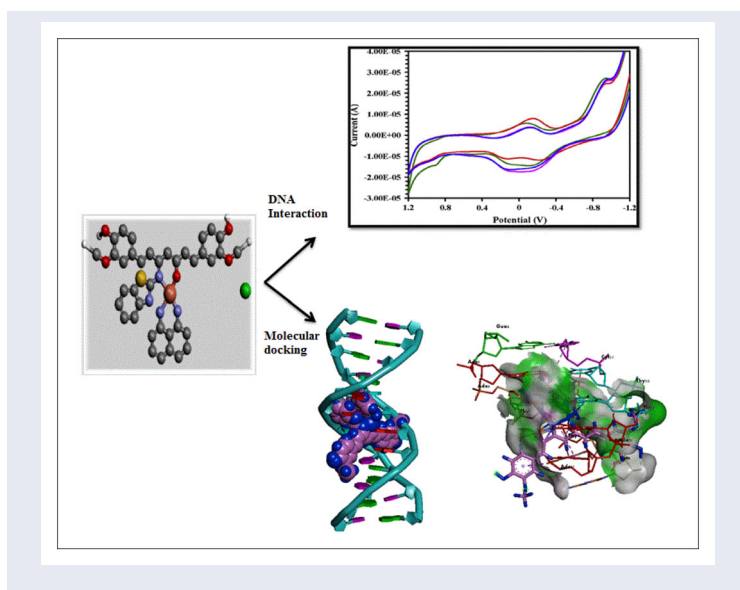
1. Introduction

There has been substantial increase in the aspire towards the discovery of effective and safe therapeutic agents for the novel drug designing due to the studies of Schiff bases and their complexes having a diverse spectrum of biological and pharmaceutical activities as antifungal [1–4], antioxidant, antibacterial [5–7] and antitumor agents [8, 9] due to their interaction to the specific sites of a DNA-strand as reactive models for protein–nucleic acid interaction, in addition to the means to develop responsive chemical probes for DNA. Thus, a number of new chemical nucleases [10–12] are synthesized which have important applications in nucleic acid chemistry, as they appear to be less readily repaired by DNA repair mechanism [13, 14] under physiological conditions and chemotherapeutic agents and in genomic research [15–19]. Schiff bases are a very important class of compounds due to their wide range of biological activities and even industrial applications [20]. Schiff bases contain the azomethine functional group, (–HC=N–) formed by the condensation of a primary amine with an active carbonyl compound [21]. This class of chelating ligands containing N, O, and S exhibits a great variety of biological activities. These activities are reported to include pharmacological applications such as antimicrobial [22], antibacterial [23], antifungal [24], antimalarial [25], antifeedant [26], antiinflammatory [27], anticancer [28], antitubercular [29], antiviral [30], anticonvulsant [31], and analgesic properties [32].

Curcumin (1,7-bis(4-hydroxy-3-methoxyphenyl)-1,6-heptadiene-3,5-dione) is an important natural phytopolyphenol found in the rhizomes of *Curcuma longa* or turmeric, which has been used in Indo-China to treat digestive and neuropsychiatric disorders [33]. The medicinal activity of curcumin has been known since ancient times. It has also been used as a photodynamic agent useful for the destruction of bacteria and tumor cells. Multiple therapeutic activities have been attributed to curcumin mostly because of

its anti-inflammatory and antioxidant effects. As such, curcumin was predominantly used to treat inflammatory conditions including bronchitis, colds, parasitic worms, leprosy, arthritis, and inflammations of the bladder, liver, kidney, and skin, and to improve symptoms such as fever and diarrhea. In addition, curcumin is thought to have beneficial effects in diseases of the neurological system including Alzheimer's disease [34].

To enhance the bustle of the potent analogue to serve as a novel drug and to eliminate adverse effects or toxicity associated with the parent drug, suitable modifications and thereby manipulating the parent structures are carried out. Metal complexes of N- and S-chelating ligands have attracted considerable attention because of their interesting physicochemical properties and pronounced biological activities. Organic compounds with heterocyclic rings having thiazole moiety are explored to have massive pharmacological and biological activities. Compounds containing benzothiazole and sulphonamide derivatives are used as antifungal, anti-inflammatory [35], anti-HIV [36], anticancer [37], anticarbonic anhydrase [38], diuretic, hypoglycaemic [39], antimalarial, and antithyroid [40] agents. Many biologically active compounds are used as drugs when administered as metal complexes possessing modified pharmacological and toxicological potentials which display increased anticancer activity [41]. The potentially used metal ions are cobalt, copper, nickel, and zinc for various pharmacological studies which have been proved to be more important biometals along with biorelevent ligands [42] due to the formation of low molecular weight complexes which are essential for normal human metabolism and its imbalance leading to excess diseases. These complexes have multiple roles in medicinal proceedings such as antimicrobial, antiviral, anti-inflammatory, enzyme inhibitors, chemical nucleases, or antitumor agents with reduced side effects and have a distinct superoxide dismutase (SOD-) mimetic activity [43, 44]. Schiff base complexes having 1,8-diaminonaphthalene (which has a planar structure and an aromatic compound) have been widely studied because of their industrial, antifungal, antibacterial, and biological applications [45–47]. The main objectives of this investigation are to design and synthesize a metal complex that shows effective DNA-binding interactions along with other biological activities. The studies provide a way towards designing an effective compound that has fewer side effects.

Hence, it is tempted to develop new pharmacological ability based complexes based on the above facts through enhancing the planarity of the coligand (1,8-diaminonaphthalene, dan), which is a bicyclic aromatic compound. The antimicrobial and DNA-binding abilities are explored in order to improve the pharmacological and anticancer efficacy. So, the synthesis and characterization of a few new curcumin-based Schiff base mixed-ligand metal(II) complexes having 1,8-diaminonaphthalene are reported in this work.

2. Experimental

Instrumentation and experimental methods of DNA binding, cleavage, and antimicrobial screening procedures are well discussed and given in Supporting Information file S1.

2.1. Synthesis of the Schiff base ligand (L)

The Schiff base (L) ligand was prepared by stirring an ethanolic solution of 10 mmol curcumin with a continuous dropwise addition of 10 mmol ethanolic solution of 2-

aminobenzothiazole. The mixture was refluxed for *ca.* 4 h. The brown solution was set aside for the evaporation of the solvent. The brown solid 4,4′-((1*E*,3*Z*,5*E*,6*E*)-5-(benzo[d]-thiazol-2-ylimino)-3-hydroxyhepta-1,3,6-triene-1,7-diyl)bis(2-methoxyphenol) (**L**) thus obtained was filtered and recrystallized from ethanol and dried in *vacuum*.

[L] Yield: 66%. Anal. Calcd. for $C_{28}H_{24}N_2O_5S$: C, 67.4; H, 4.9; N, 5.3. Found: C, 67.3; H, 4.3; N, 5.1. IR (KBr pellet), ν (cm^{-1}): 1643 ν(–C=N); 1520, ν(–HC=C); ^{1}H NMR, δ (ppm): 6.1–8.2 (m) (aromatic); 5.4 (–OH); 7.8 (–C=CH–1H) (s); 3.6 (-OCH$_3$) (s); 16.9 (s) (-OH, enol). ^{13}C NMR δ (ppm): 56.1 (C$_1$), 149.1 (C$_2$), 147.9 (C$_3$), 116.8(C$_4$), 129.9 (C$_5$), 111.9 (C$_6$), 119.5 (C$_7$), 184 (C$_8$), 82 (C$_9$), 164.6 (C$_{10}$), 174.6 (C$_{11}$), 148.71 (C$_{12}$), 121.6 (C$_{13}$), 125.3 (C$_{14}$), 124.5 (C$_{15}$), 121.8 (C$_{16}$), 125.8 (C$_{17}$). UV-vis in DMF, λ_{max} (nm): 225, 349.

2.2. Synthesis of mixed-ligand metal(II) complexes

To an ethanolic solution of the Schiff base (L) (10 mmol), an ethanolic solution of metal(II) chloride of copper/nickel/cobalt/zinc (10 mmol) was added with stirring and refluxed for 5 h after the addition of 1,8-diaminonaphthalene in ethanol (10 mmol). After cooling the reaction mixture to room temperature, the formed solid was filtered, washed with ethanol and then with petroleum-ether, and was finally dried in *vacuum* at room temperature.

[CuL(dan)]Cl (1): Yield: 66%. Anal. Calcd. for $C_{38}H_{33}ClN_4O_5SCu$: C, 60.3; H, 4.4; N, 7.4; Cu, 8.4. Found: C, 60.2; H, 4.3; N, 7.3; Cu, 8.3%. IR (KBr pellet), ν(cm^{-1}): 1634 ν(–C=N); 1527 ν(–HC=C); 415 ν(M–N), 523 ν(M–O). Λ_M (Ω^{-1} cm^2 mol^{-1}) = 75.3. UV-vis in DMF, λ_{max} (nm): 231, 322 and 538. μ_{eff} (BM): 1.72.

[CoL(dan)]Cl (2): Yield: 59%. Anal. Calcd. for $C_{38}H_{33}ClN_4O_5SCo$: C, 60.7; H, 4.4; N, 7.5; Co, 7.8. Found: C, 60.6; H, 4.3; N, 7.4; Co, 7.7%. IR (KBr pellet), ν (cm^{-1}): 1630 ν(–C=N); 1510 ν(–HC=C); 434 ν(M–N), 522 ν(M–O). Λ_M (Ω^{-1} cm^2 mol^{-1}) = 79.3. UV-vis in DMF, λ_{max} (nm): 271, 345 and 574. μ_{eff} (BM): 3.5.

[NiL(dan)]Cl (3): Yield: 61%. Anal. Calcd. for $C_{38}H_{33}ClN_4O_5SNi$: C, 60.7; H, 4.4; N, 7.4; Ni, 7.8; Found: C, 60.6; H, 4.3; N, 7.3; Ni, 7.7%. IR (KBr pellet), ν (cm^{-1}): 1620 ν(–C=N); 1521 ν(–HC=C); 440 ν(M–N), 526 ν(M–O). Λ_M (Ω^{-1} cm^2 mol^{-1}) = 74.2. UV-vis in DMF, λ_{max} (nm): 258, 351 and 518. μ_{eff} (BM): diamagnetic.

[ZnL(dan)]Cl (4): Yield: 67%. Anal. Calcd. for $C_{38}H_{33}ClN_4O_5SZn$: C, 60.2; H, 4.4; N, 7.39; Zn, 8.6. Found: C, 60.1; H, 4.3; N, 7.1; Zn, 8.5%. IR (KBr pellet), ν (cm^{-1}): 1626 ν(–C=N); 1711 ν(–C=O), 1520 ν(–HC=C); 445 ν(M–N), 520 ν(M–O). ^{1}H NMR, δ (ppm): 6.9–8.2 (aromatic) (m); 5.6 (–OH); 6.04 (–C=CH–1H) (s); 3.8 (-OCH$_3$); ^{13}C NMR, δ (ppm): 56.1 (C$_1$), 149.1 (C$_2$), 147.9 (C$_3$), 116.8(C$_4$), 129.9 (C$_5$), 111.9 (C$_6$), 119.5 (C$_7$), 184 (C$_8$), 82 (C$_9$), 164.6 (C$_{10}$), 174.6 (C$_{11}$), 148.71 (C$_{12}$), 121.6 (C$_{13}$), 125.3 (C$_{14}$), 124.5 (C$_{15}$), 121.8 (C$_{16}$), 125.8 (C$_{17}$), 148.4 (C$_{18}$), 122.7 (C$_{19}$), 127.4 (C$_{20}$), 128.3 (C$_{21}$), 133.7 (C$_{22}$). Λ_M (Ω^{-1} cm^2 mol^{-1}) = 76.7. UV-vis in DMF, λ_{max} (nm): 270, 367. μ_{eff} (BM): diamagnetic.

3. Results and discussion

The novel biologically potent Schiff base and its mixed-ligand metal(II) complexes are synthesized according to the synthetic route depicted in Scheme 1. They are stable in air. The ligand is soluble in general organic solvents but the metal(II) complexes are
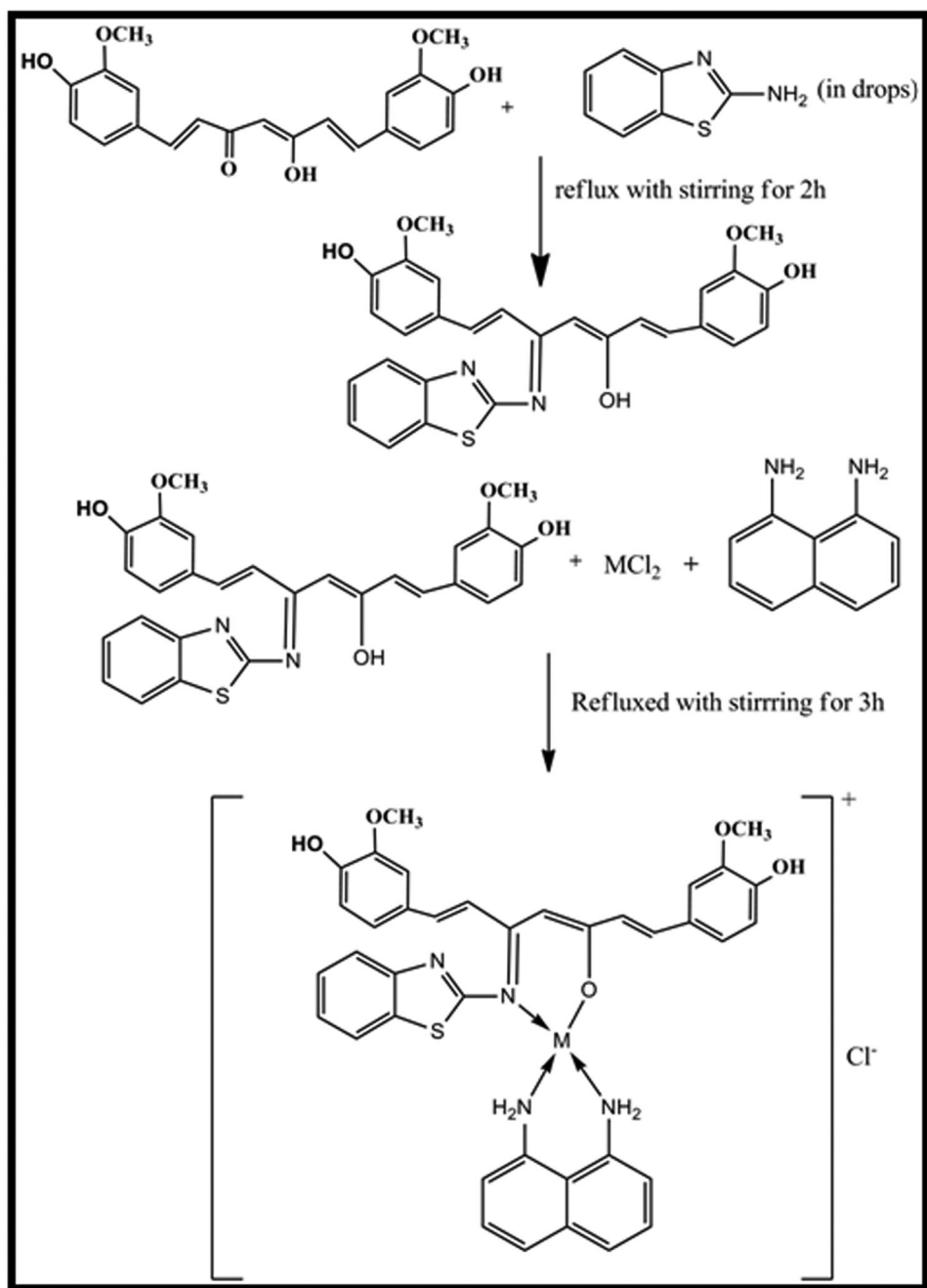
Scheme 1. Synthesis of Schiff base ligand and its mixed ligand metal(II) complexes.

soluble only in DMF and DMSO. The magnetic susceptibility data reveal that copper(II) and cobalt(II) complexes are paramagnetic while nickel(II) and zinc(II) complexes are diamagnetic in nature. The analytical and physical data of the synthesized compounds are shown in Supporting Information Table S1.

3.1. Infrared spectra

A precious correlation on the nature of the coordination and site of coordination of the ligand to the metal ion is known from the data of IR spectra of the free ligand with the complexes. A strong broad band observed in the region 3440–3365 cm^{-1} for both the free ligand (L) (Supporting Information Figure S1(a)) and the copper(II) complex (Supporting Information Figure S1(b)) is allocated to phenolic -OH group of curcumin moiety which is an inference that phenolic OH group is not in coordination. The IR spectrum of the ligand shows a weak broad band at 3150–2950 cm^{-1} which is assigned to enolic − OH group of curcumin. The weak and broadness of this peak is mainly due to the intramolecular hydrogen bonding between the enolic –OH group with ketonic group of curcumin and due to stabilization of –OH group by the conjugation with -C$=$O present in the curcumin system. The absence of enolic –OH group in Schiff base ligand is due to the formation of − C$=$N between the curcumin and the 2-aminobenzothiazole which hinders the keto-enol tautomerism [48]. In addition, the − C$=$N present in the thiazole ring of 2-aminobenzothiazole of the complex and the free ligand at 1556 cm^{-1} is a sign of non-involvement of nitrogen atom of thiazole moiety in coordination [49]. The Schiff base shows a strong band at 1643 cm^{-1} which is ascribed to − C$=$N group. This region is expected to absorb at lower frequency in the complexes and the same is observed in 1620–1634 cm^{-1} for the complexes due to possible float of the lone pair electron density towards the metal ion and makes a strong evidence for the coordination of − C$=$N through nitrogen to the metal ion. Furthermore, new peaks observed in the metal complexes in the regions 415–445 cm^{-1} and 520–526 cm^{-1} are assigned to M-N and M-O, respectively. The IR spectral data of Schiff base ligand and the metal(II) complexes are tabulated in Supporting Information Table S2.

3.2. Molar conductivity

The observed molar conductance values of the complexes (74.2–79.3 Ω^{-1}cm^{-2}mol^{-1}) support their electrolytic nature. The elemental analysis outcome of the metal complexes also agrees with the calculated values, showing that the complexes have 1:1:1 metal:ligand:coligand ratio.

3.3. Magnetic moments and electronic spectra

The geometry of the metal complexes has been construed from the absorption spectra and magnetic data. The free ligand exhibits two intense bands at 224.6 and 348.6 nm corresponding to $\pi \rightarrow \pi^*$ and $n \rightarrow \pi^*$ transitions, respectively. In all the metal complexes, the absorption bands at 231–271 and 322–367 nm are due to $\pi \rightarrow \pi^*$ and $n \rightarrow \pi^*$ transitions that are observed in the spectrum of the free ligand (L). The values are tabulated in Supporting Information Table S3. These transitions are shifted to upfield or downfield frequencies due to coordination of the ligand with metal ions. The cobalt and copper complexes show d-d bands, respectively, at 574 and 538 nm that strongly favor the square planar geometry around the metal ions, which are assigned to the combination of $^1A_{1g} \rightarrow {}^1B_{1g}$ and $^2B_{1g} \rightarrow {}^2A_{1g}$ transitions, respectively,

ensuring the geometry of the complexes to be square planar. The electronic absorption spectrum of Cu(II) complex is shown in Supporting Information Figure S2. The Cu(II) and Co(II) complexes are magnetically normal with a magnetic moment of 1.72 and 3.5 BM, respectively. The observed diamagnetic nature of the Ni(II) complex confirms the square planar geometry. The Zn(II) complex exhibits intraligand charge transfer transitions. It is expected to be diamagnetic, as expected for d^{10} configuration. The basic structure of the monomeric complex is further determined by microanalytical and mass spectral data. These values are comparable with other reported complexes [50, 51]. However, the exact geometry will be confirmed only from the X-ray single-crystal study. The minute size of the compound is a hindrance for the growth of single-crystal and hence we are abortive to develop suitable single crystal.

3.4. NMR spectrum of zinc(II) complex

In ^{1}H NMR spectra, the phenolic –OH and –OCH$_3$ protons for ligand (L) and the zinc(II) complex (represented in Supporting Information Figures S3(a) and S3(b)) are observed as a singlet at 5.4 ppm and 3.7 ppm, respectively, in curcumin moiety which is inference of the non-involvement of phenolic –OH and–OCH$_3$ protons in coordination to the metal ion. The appearance of a new peak in the zinc complex at 8 ppm reveals that the amino group of 1,8-diaminonaphylene is coordinated to the metal ion.

The ^{13}C NMR spectrum of the ligand shows aromatic carbons at 111.9–149.1 ppm. The ligand also exhibits the C=N carbon at 168.7 ppm, which is shifted to 164.6 ppm (Supporting Information Figure S4) upon coordination, indicating that the C=N group participates in complex formation. The ligand also shows peaks for –C-OH at 185.4 ppm which is shifted towards downfield 182.5 ppm, indicating the coordination of –C-O with Zn(II) ion. The appearance of new bands in the Zn(II) complex at 148.4, 122.7, 127.4, 133.7, and 133.9 ppm shows the coordination of 1,8-diaminonaphthalene to the Zn(II) ion.

3.5. EPR spectra

The EPR spectrum of the Cu(II) complex recorded in DMSO (0.1 M) gives valuable information. There is an intense band in the region of high field. From the g tensor value of the copper complex, the ground state has been derived. In the square planar complexes, the unpaired electron lies in the d_{x2-y2} orbital giving that the ground state as $^2B_{1g}$ with $g_{||} > g_{\perp} > 2$. From these calculated values for the Cu(II) complex (Supporting Information Figure S5), the magnitude of the spin Hamiltonian parameters and bonding parameters of the copper(II) complex has been estimated and are tabulated in Supporting Information Table S4. It is obvious that $A_{||} > A_{\perp}$ and $g_{||} > g_{\perp} > 2$ recommending that all the complexes are square planar geometry and the system is axially symmetric [52]. In the complex, the unpaired electron is in d_{x2-y2} orbital making the ground state as $^2B_{1g}$. The calculated G value [$G = (g_{||} - 2)/(g_{\perp} - 2)$] is 5.0, confirming that the unpaired electron is present predominantly in d_{x2-y2} orbital.

The G value is a measure of exchange interaction between the copper centers in polycrystalline solid which is calculated to be 5.0, indicating negligible exchange interaction of Cu–Cu in the complex according to Hathaway [53].

The bonding parameters α^2 and β^2 have been evaluated for the Cu(II) ion with the ligand. Field environment is regarded as a measure of in-plane bonds (α^2 and β^2) and out-of-plane bond (π^2). There is some considerable interaction in out-of-plane π-bonding and the in-plane π-bonding which is purely ionic. The $g_{\parallel}/A_{\parallel}$ value is $170\,cm^{-1}$, which is in harmony with significant deviation from planarity and confirmed by the bonding parameter α^2 value which is less than unity. The covalency parameters, covalent in-plane σ-bonding (α^2) and covalent in-plane π-bonding (β^2) have been calculated using the following equations:

$$\alpha^2 = (A_{\parallel}/0.036) \;+\; (g_{\parallel}-2.0027) \;+\; 3/7\,(g_{\perp}-2.0027) \;+\; 0.04$$
$$\beta^2 = (g_{\parallel}-2.0027)\,(E/-8\alpha\lambda^2)$$

If the value of α^2 is 1.0, it indicates the complete ionic character, whereas if $\alpha^2 = 0.83$, it denotes 100% covalent bonding, with the hypothesis of negligible small value of the overlap integral. The α^2 and β^2 values indicate that there is a considerable interaction in the in-plane σ-bonding whereas the in-plane π-bonding is almost ionic. Comparing to β^2 value, the α^2 is lower than β^2 revealing that the in-plane σ-bonding is more covalent than in-plane π-bonding. The above observations confirm the square planar geometry of the complex. Thus, the EPR study of the Cu(II) complex has provided supportive evidence to the conclusion obtained on the basis of electronic and magnetic moment values.

3.6. Mass spectra

The ESI-mass spectra of synthesized Schiff base ligand and the copper(II) complex recorded at room temperature confirm the proposed stoichiometry. The obtained molecular ion peaks confirm the suggested formulas for the synthesized compounds. The spectrum of L (Supporting Information Figure S6(a)) showed a molecular ion peak $[M^+]$ at $m/z = 500$ equivalent to its molecular weight, corresponding to its molecular formula, $C_{28}H_{24}N_2O_5S$. In addition to this, the fragmentation peaks observed at m/z 148, 358, 149, and 55 are due to the cleavage of $[C_7H_4N_2S_2]^+$, $[C_{21}H_{20}O_5]^+$, $[C_9H_9O_2]^+$, and $[C_3H_3O]^+$, respectively. These results confirm the formation of Schiff base L and support the IR and NMR results. Its Cu(II) complex **1** (Supporting Information Figure S6(b)) showed a molecular ion $[M^+]$ at m/z 756, equivalent to its molecular weight having the formula $C_{38}H_{31}CuN_4O_5S$. Therefore, the mass spectral and the elemental analyses data conjointly agree with the formation of [M(L)(dan)]Cl type complexes of 1:1:1 stoichiometry. The spectra of **2**–**4** showed molecular ion peaks at $m/z = 753$ $[M^+]$, 752 $[M^+]$, and 759 $[M^+]$, respectively. All these fragments are leading to formation of the species [M(L)]Cl, which further undergoes de-metalation to yield the species (L) giving the fragment ion peak at $m/z = 500$ as expected. Thus, the mass spectral data of the complexes reinforce the observed elemental analytical and other observed data.

3.7. DNA Interaction

3.7.1. Complex stability in buffer solution

The stability of the complexes in 5% DMSO solution of Tris–HCl buffer at 7.2 pH has been assessed by UV-vis spectrophotometry. Only a little change in absorbance exhibits no intraligand band shifts after 3 days. This small change in absorbance without any significant shift in wavelengths (λ_{max}) predicts the stability of these complexes in the above buffer solution. However, a slight change in the intensity of these absorption bands is observed but there is no formation of any precipitate during this time period. These results indicate the strong nature of the complexes. Hence, these findings indicate that our complexes are sufficiently stable in the Tris–HCl buffer environment even after reaching DNA.

3.7.2. Electronic absorption titration with CT-DNA

The electronic absorption titration is an adaptable tool for the studies of DNA-binding with the metal complexes through the variation in the absorbance. The shift in the wavelength in the UV-vis region with the addition of CT-DNA to the complexes' solution indicates the nature of interaction of the complexes with CT-DNA.

The transition metal complexes are approved to bind with DNA either *via* both covalent and noncovalent or noncovalent interactions [54]. The noncovalent DNA interactions comprise: (i) major or minor grooves of DNA double helix, (ii) electrostatic interactions with the negatively charged nucleic sugar phosphate structure, which are along the external DNA double helix and do not possess selectivity, and (iii) intercalation between the stacked base pairs of native DNA [55]. The labile ligand of the metal complexes is substituted by a nitrogen base during covalent binding of DNA with the complexes. Both hypochromism and hyperchromism are the spectral features of DNA concerning its double helix structure. The DNA binding mode of a complex *via* electrostatic effect or intercalation marks as hypochromism while hyperchromism point towards the breakage of the secondary structure of DNA on binding with the complex. The absorption spectra of the complexes in the absence and presence of CT-DNA (at constant concentration of the complex) are shown in Figure 1.

The absorption spectra of the complexes display an intense intraligand π-π^* absorption band for all metal complexes in the range 321–334 nm in UV region which has been selected to examine the variation of absorption band due to the binding interaction of DNA with the metal complexes. On addition of the same amount of DNA, metal complexes show hypochromism along with a slight red-shift charge transfer peak maxima in the electronic absorption spectra of the metal complexes. The empirical hypochromicity values in the presence of DNA are in the range 14.6–21.5% for LMCT band and their red-shifts are observed in the region 2–4 nm which substantiate the binding of DNA with the complexes is through intercalative mode [56].

The spectral characteristics infer that the complexes interact with CT-DNA through intercalative binding mode. Hypochromism and bathochromism in electronic absorption titration may be attributed to the intercalation binding nature of complexes with DNA and the participation of stacking interactions between aromatic chromosphores and the base pairs of DNA which cause the π^* orbital of the intercalated ligand to couple with the π orbital of the base pairs of DNA and due to the decrease of π-π^*
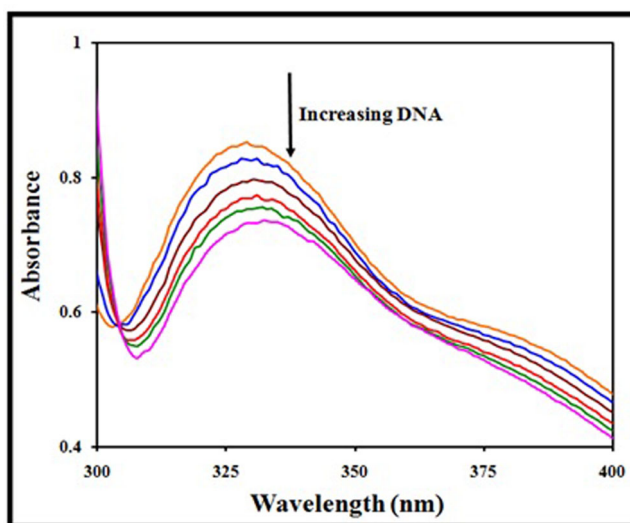
Figure 1. Absorption spectrum of [CuL(dan)]Cl in buffer pH = 7.2 at 25 °C in the presence of increasing amount of DNA.

**Table 1.** Electronic absorption spectral data of complexes.

| Complexes | λ_{max} (nm) | | $\Delta\lambda$ (nm) | %H^a | ^bK_b (M^{-1}) × 10^{-4} |
	Free	Bound			
[CuL(dan)]Cl	329.0	333.0	4.0	21.5	3.9 ± 0.05
[CoL(dan)]Cl	327.0	331.0	3.0	18.6	3.5 ± 0.08
[NiL(dan)]Cl	321.0	323.0	2.0	15.2	2.9 ± 0.04
[ZnL(dan)]Cl	334.0	336.0	2.5	14.6	2.4 ± 0.07

$^aH\% = [(A_{free} - A_{bound})/A_{free}] \times 100\%$.
^bK_b = Intrinsic DNA binding constant determined from the UV-Vis absorption spectral titration.

transition energy which marks in the bathochromism. Hypochromism and bathochromism are noteworthy due to π-stacking or hydrophobic interactions of the planar aromatic phenyl rings [55]. The coupling of partially filled π^* orbital decreases transition probabilities, thus resulting in the hypochromism [42].

The slope to intercept ratio from the plot between [DNA]/($\varepsilon_b - \varepsilon_f$) *versus* [DNA] is given in Table 1, which is used to determine the intrinsic binding constant (K_b) values and used to collect the information regarding binding affinity of the complexes with CT-DNA. Comparing the K_b values of the metal complexes with the classical intercalator, the complexes have lesser binding affinity than the classical intercalator Ru(II) complexes. From the intrinsic binding constant (K_b) values, the ligand is a feeble intercalator as compared to the metal complexes which act as strong intercalators. The strong binding affinity of the metal complexes to the CT-DNA is a result of auxiliary π-π^* interaction of the planar aromatic phenyl rings and central metal ions as compared to the Schiff base ligand, also drastically promoted due to effective release of the ligand (L), higher planar area, extended π-system, the coordination of amino acid moiety and aromaticity between two intact base pairs. On comparison among all metal complexes, Cu(II) complex exhibits an effective intercalation and the order of intercalation is given by the decreasing order of the intrinsic binding constant (K_b) values which is Cu(II) > Zn(II) > Co(II) > Ni(II) [41].
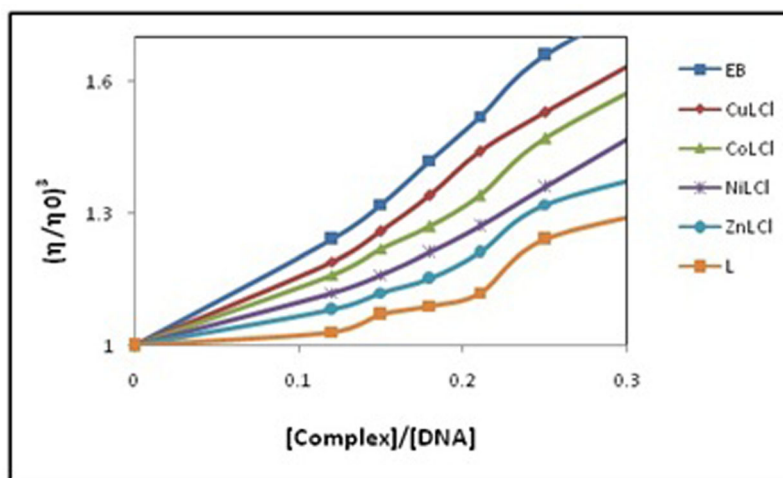
Figure 2. Effect of increasing amounts of [EB], [CuL(dan)]Cl, [CoL(dan)]Cl, [NiL(dan)]Cl, and [ZnL(dan)]Cl on the relative viscosity of DNA. 1/R = [Complex]/[DNA] or [EB]/[DNA].

3.7.3. Viscosity measurements

For the determination of the DNA-binding mode, viscosity is the most conclusive and the least obscure method [57]. As the intercalation mode occurs between DNA and the binding agent, an obvious separation of the base pairs can be detected by measuring the relative specific viscosity [58]. The interaction of the macrocyclic metal(II) complexes with CT-DNA is prop up by viscosity measurement of DNA and regarded as the most decisive test for DNA-binding mode in solution in the absence of crystallographic data. To explore the interaction of CT-DNA with the complexes, the relative specific viscosity of CT-DNA has been calculated by altering the concentration of the metal complexes. The intercalating agents such as ethidium bromide (EB) cause a significant increase in the viscosity of a DNA solution under suitable conditions. The conservative intercalation model demands the lengthening of DNA-helix as base pairs that are unconnected to accommodate the binding of ligand and consequently there is an increase in the overall DNA contour length, as shown in Figure 2. By increasing ratio of the metal complexes to DNA, the viscosity of DNA solution increased. Weighing against EB, the complexes demonstrate slight increase in the relative viscosity of CT-DNA with an ominous intercalation mode between the complex and DNA. This outcome recommends an intercalating binding mode of the complexes with CT-DNA and corroborates the electronic spectroscopic results, hypochromism and red-shift of the complexes in the presence of DNA. The viscosity studies provide a strong substantiation for intercalation and these studies credit the intercalative binding mode of the drug that could cause the effective length of the DNA to increase [59].

3.7.4. Effect of CT-DNA on cyclic voltammetry

The nature of binding of the complexes to the CT-DNA is further explored by cyclic voltammetry (CV), not only constructive in probing the nature and mode of DNA-binding of metal complexes but also provides the relative account on nature of interacting species. The application of electrochemical methods in the study of
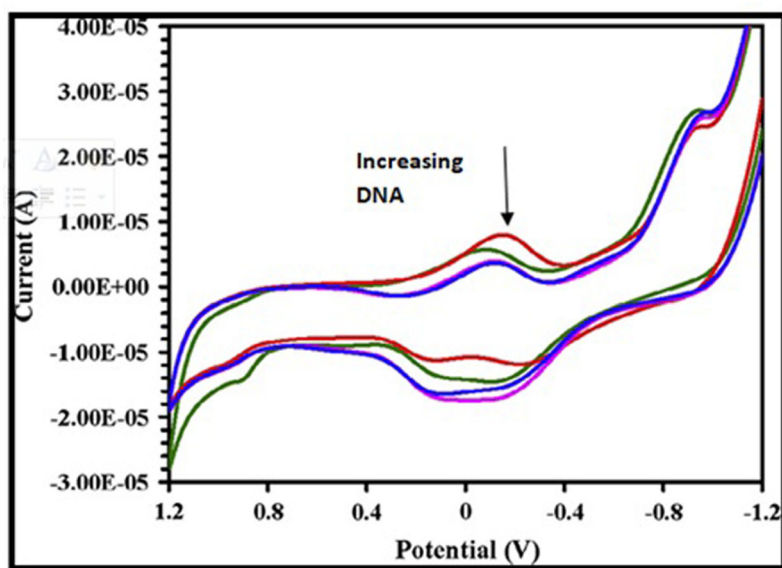
Figure 3. Cyclic voltammogram of [CuL(dan)]Cl in buffer pH = 7.2 at 25 °C in the presence of increasing amount of DNA.

Table 2. Redox potential profiles for interaction of DNA with metal(II) complexes.

| Complexes | [a]ΔE_p (V) | | [b]$E_{1/2}$ (V) | | Ip_a/Ip_c |
	Free	Bound	Free	Bound	
[CuL(dan)]Cl	0.568	0.623	0.540	0.556	0.92
[CoL(dan)]Cl	0.712	0.825	0.512	0.529	0.89
[NiL(dan)]Cl	0.458	0.512	−0.256	−0.210	0.76

Data from cyclic voltammetric measurements.
[a]$E_{1/2}$ is calculated as the average of anodic (E_{pa}) and cathodic (E_{pc}) peak potentials: $E_{1/2} = E_{pa} + E_{pc}/2$.
[b]$\Delta E_p = E_{pa} - E_{pc}$.

metallointercalation and coordination of transition metal complexes to DNA provides a useful complement to electronic spectral titration [60, 61] and viscosity studies. The characteristic CV behavior of the Cu(II) complex in the absence and presence of CT-DNA altering amount of DNA is shown in Figure 3.

The metal(II) complexes reveal a shift in the anodic and cathodic peak potentials followed by decrease in peak currents, demonstrating the intercalating interaction existing between the metal(II) complexes and CT-DNA. Table 2 offers the calculated shifts of the cathodic (E_{pc}) and anodic (E_{pa}) potentials and quasi reversible redox couples upon the addition of CT-DNA in Tris-HCl and NaCl buffer solution to the Cu(II), Co(II), and Ni(II) complexes in DMSO. The voltammetric current of the redox wave drops on the addition of DNA with a slight shift in $E_{1/2}$ to positive potential, which also signifies the degree of binding affinity of the complex with DNA. The diffusion of the metal complex bound to the large, slowly diffusing DNA molecule [58] may be approved by the fall of voltametric currents with the addition of DNA to the metal complex. The grid shift in $E_{1/2}$ can be used to calculate the ratio of equilibrium binding constants according to the model of interaction illustrated by Carter and Bard. Significant reduction in the current intensity of all peaks and migration of redox

Table 3. Minimum inhibitory concentration of the synthesized compounds against the growth of bacteria.

| Compounds | Minimum inhibitory concentration (MIC) ($\times 10^4$ µM) | | | | |
	Staphylococcus aureus	Bacillus subtilis	Escherichia coli	Pseudomonas aeruginosa	Salmonella typhi
L	15.3	14.1	13.3	14.6	16.6
Dan	15.0	14.0	13.2	14.4	16.3
[CuL(dan)]Cl	9.3	9.5	10.4	10.8	12.5
[CoL(dan)]Cl	12.1	11.7	11.5	11.6	12.3
[NiL(dan)]Cl	13.1	12.9	13.6	13.1	14.1
[ZnL(dan)]Cl	12.6	12.9	13.5	13.7	13.9
[a]Kanamycin	1.6	2.8	1.4	2.3	2.6

[a]Kanamycin is used as the standard.
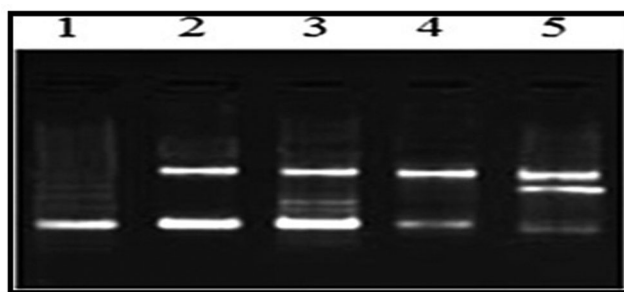
Figure 4. Gel electrophoresis pattern showing cleavage of pBR322 supercoiled DNA (10 µM) in the presence of H_2O_2 (100 µM); Lane 1: DNA control (10 µM); lane 2: DNA + Zn(II) complex (60 µM) + H_2O_2; lane 3: DNA + Ni(II) complex (60 µM) + H_2O_2; lane 4: DNA + Co(II) complex (60 µM) + H_2O_2; lane 5: DNA + Cu(II) complex (60 µM) + H_2O_2.

couple towards the positive side is a representation that the complex binds to DNA through intercalation mode of binding [62].

3.7.5. DNA-cleavage study

The DNA-cleavage efficiency of the complexes induced by hydrogen peroxide as oxidant has inspired researchers to keep synthesizing a variety of metal complexes that effectively cleave DNA molecule either with hydrolytic or oxidative pathways due to the importance of DNA cleavage in pharmaceutical and biotechnological applications. The DNA-cleavage efficiency induced by ligand and the complexes in the presence of H_2O_2 has been characterized by using pBR322 circular plasmid DNA. At micromolar concentration for an incubation time of 2 h, the ligand demonstrates temperate cleavage activity in the presence of the oxidant (H_2O_2). The delivery of metal ion to the DNA helix, in locally generating oxygen or hydroxide radicals, capitulates a well-organized DNA cleavage reaction. Figure 4 illustrates the gel electrophoretic separations in screening the cleavage activities of pBR322 DNA induced by metal complexes. In Figure 4, lane 1 is control while the other lanes contain compounds in the presence of H_2O_2 as oxidant. It is apparent that the parent ligand shows a visible cleavage activity in the presence of the oxidant. The other lanes contain DNA-cleavage, analyzed by monitoring the conversion of form I (super coiled) converted into form II (nicked) and form III (linear). The relative DNA-cleavage efficacy of the complexes is significantly increased in the presence of the oxidant (H_2O_2) due to the formation of hydroxyl free

radicals, which oxidize metal ion from +2 to +3 through Fenton-type reactions which results in the generation of reactive oxygen species that causes the oxidative damage to DNA: ($H_2O_2 + M^{n+} \rightarrow M^{n+1} + \bullet OH + OH^-$).

It is found that the complexes are the most powerful nuclease imitates in terms of molecular structure. On account of the geometrical structures and chemical environment these complexes with H_2O_2 play an efficient role as found to be efficient oxidant and as nucleolytic molecules. The different DNA-cleavage efficiency of the complexes may be considered due to the different binding affinity to DNA.

3.8. In vitro biological studies

3.8.1. Antibacterial activity

The prepared ligand and the metal complexes have been tested for their *in vitro* antimicrobial activity against the five strains of bacteria (Gram-negative and Gram-positive) because bacteria can achieve resistance to antibiotics through biochemical and morphological modifications [63]. The minimal inhibitory concentrations of tested complexes against certain bacteria are displayed in Table 3. The metal complexes of the functionalized β-ketimine show elevated *in vitro* antibacterial activity. The obtained MIC values reflect that all metal complexes reveal substantial bactericidal activities compared to Schiff base which has a moderate activity, but their activities are lower than the standard drugs. The significant activity of the Schiff base ligand may occur due to the presence of imine group which explicates the mechanism of transformation reaction in biological systems. The increased activity of the complexes is more pronounced when the Schiff base is coordinated to the metal ion. The nature of metal ion in the complexes also plays a crucial role in determining antimicrobial properties, hence it is induced by using either a biocation or a metallic ion exhibiting inhibitory properties.

In the present study, the order of the antimicrobial activity of the synthesized compounds is Cu(II) > Co(II) > Ni(II) > Zn(II). The studies reveal that the copper complex has effective and direct impact on selective antimicrobial activities against bacteria. The higher activity of the copper complex than other metals is deduced from the fact that increases in the size of the metal ion decreases the polarization. The vital features of antimicrobial activities can be correlated as follows: (i) the presence of uncoordinated heteroatoms such as N, O, and S which increase the activity of the complexes by bonding with trace elements present in microorganisms that enhance the solubility (hydrophilic or hydrophobic), thus are inhibiting the growth of microorganism, (ii) the mode of action of the complexes involve the capability to form hydrogen bonding of the hydroxyl group with a counter anion or solvent molecules, the active centers of cell constituents ensuing in the meddling of the cell metabolism [64].

3.8.2. Antifungal activity

To enhance the medicinal scope in the field of bioinorganic chemistry, the synthesized metal complexes have been evaluated for their antifungal actions evaluated using the disk diffusion method. The Schiff base ligand and the metal complexes have been screened *in vitro* to facilitate the antifungal activities against *Aspergillus niger*, *Fusarium*

Table 4. Minimum inhibitory concentration of the synthesized compounds against the growth of fungi.

|	Minimum inhibitory concentration (MIC) ($\times 10^4$ μM)				
Compounds	Aspergillus niger	Fusarium solani	Curvularia lunata	Rhizoctonia bataticola	Candida albicans
L	16.3	15.7	`16.2	15.2	17.6
Dan	14.3	15.1	15.5	14.7	16.4
[CuL(dan)]Cl	9.7	9.5	11.8	11.3	10.6
[CoL(dan)]Cl	12.7	11.3	12.4	12.9	12.0
[NiL(dan)]Cl	15.1	13.3	13.6	13.7	13.1
[ZnL(dan)]Cl	15.5	14.1	14.8	15.1	14.3
[a]Fluconazole	1.3	1.8	1.1	1.4	1.7

[a]Fluconazole is used as the standard.

solani, *Culvularia lunata*, *Rhizoctonia bataticola*, and *Candida albicans*. The outcome of the antifungal studies is tabularized in Table 4, which discloses that the metal complexes are more toxic than the free ligand against the same organisms. The enhancement in the antifungal activity of the metal complexes is due to the inhibition of replication process of the microbes by blocking their metabolic active sites. Such increased activity can be explained on the basis of Tweedy's chelation theory [65]. The chelation also increases the lipophilic nature and an interaction between the metal ion and the lipid, thus blocking of the metal binding sites in the enzymes of microorganisms is favored. This may lead to perturb of the permeability of cell respiration process, thus resulting in interference with the normal cell processes which blocks the synthesis of proteins. Antimicrobial activity is an obscure blend of several aspects such as nature of the metal ion and the ligand, the geometry of the metal complexes, their lipophilicity, the steric and pharmacokinetic factors which also play a vital role along with chelation [66].

3.9. Molecular docking

Molecular docking has become an increasingly important tool for drug discovery. It is a powerful approach for structure-based drug discovery. The assimilation of computational and experimental strategies has been of big value in the recognition and development of new promising compounds. This strategy estimates the ligand-receptor binding free energy by evaluating critical phenomena involved in the intermolecular recognition process. Molecular docking approach is mostly used in drug discovery and medicinal chemistry. In this study, the binding free energy of the synthesized ligand and its metal complexes are predicted by using HEX 8.0 software against nucleic acid (PDB ID: 1BNA) receptor molecule. The binding model and hydrogen bond interactions of the examined compounds are displayed by Discovery studio visualized. The binding energy of compounds in molecular docking should be low as the parameters are represented in negative scores i.e. as integers. Thus, the more negative the relative binding, the more potent the binding between DNA and target molecules. All the metal complexes have potent to bind with receptor than the ligand. Docking score of the ligand is 334.14 kJ mol^{-1} and its complexes are 360.00 (Cu(II)), 350.20 (Co(II)), 348.76 (Ni(II)), and 345.04 (Zn(II)) kJ mol^{-1}, respectively. When binding energy has high negative value, the binding of complexes with 1BNA receptor is greater. Thus, if the
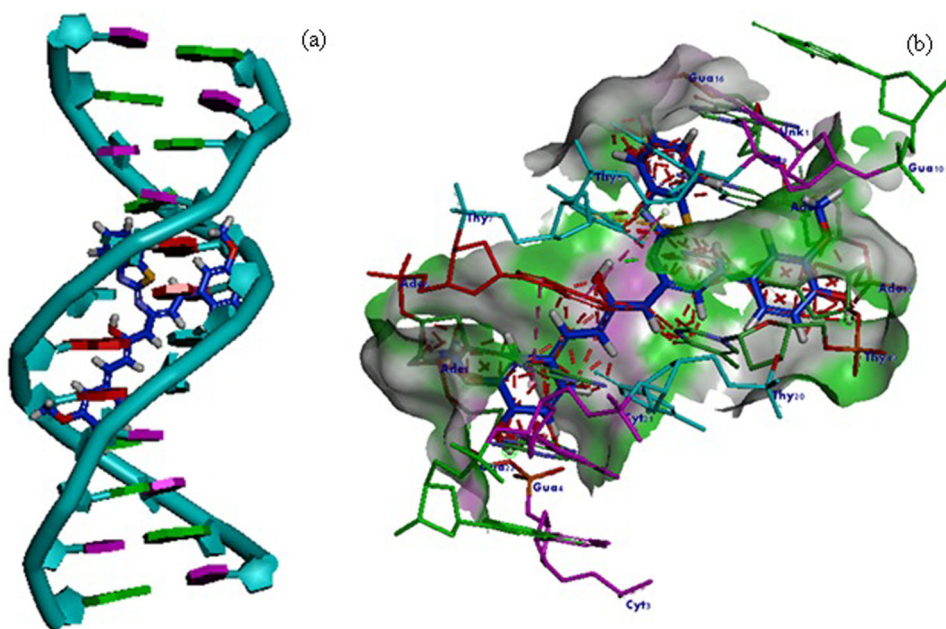
Figure 5. Binding model of ligand (a) and its H-bonding interactions (b).
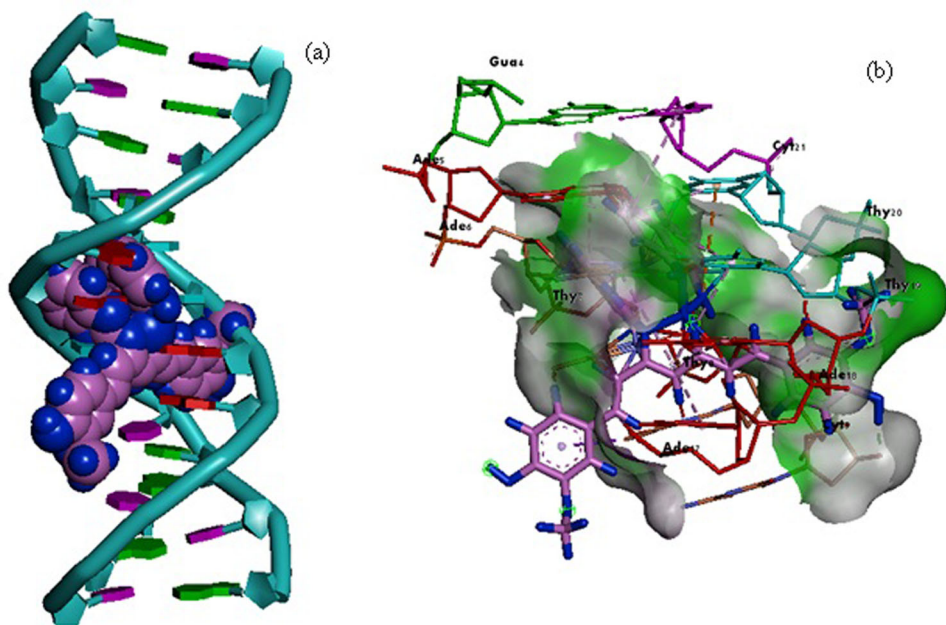
Figure 6. Binding model of Co(II) complex (a) and its H-bonding interactions (b).

binding energy is lower it means the compound possesses higher rate of binding with the DNA. The complexes are less potent than the few reported complexes, which may be due to the enhancement in the planarity of the co-ligand where the nitrogen is

attached within the plane wherein 1,8-diaminonapthalene is attached in the side chain of the naphthalene ring moiety [67, 68]. The binding model of synthesized ligand and its Co(II) complex with 1BNA receptor is shown in Figures 5 and 6.

4. Conclusion

Metal complexes which show promising results afford a platform for the opportunities to develop metal and metal-based drug aspirant in the discovery and development of innovative novel therapeutic agents. Therapeutic activities of the compounds can be increased by the formation of complex with different metal ions. In this report, coordination chemistry of a Schiff base ligand obtained from the reaction of curcumin with 2-aminobenzothiazole has been described. The metal complexes of Schiff base ligand with Cu(II), Ni(II), Co(II), and Zn(II) along with 1,8-diaminonaphthalene as co-ligand have been synthesized and characterized by spectral and analytical data. Based on spectral data, the geometry assigned to the complexes is square planar. The metal complexes have superior antimicrobial activity than the ligand. The *in vitro* DNA-binding study of the complexes with CT–DNA has been explored. Biophysical and spectroscopic techniques of DNA binding studies reveal that the Cu(II) complex has highest propensity for DNA binding than the other studied metal complexes. The DNA-binding mode is effectively inferred to be intercalative mode of interaction. Furthermore, the DNA-cleavage activity of metal complexes has been performed by agarose gel electrophoretic assay. The complexes exhibit effective DNA-cleavage *via* hydrolytic mechanistic pathway and hence the complexes have been developed as novel DNA hydrolytic cleavage agents. It is found that the biological activity and the binding ability of the synthesized metal complexes are potent. The reason may be due to the presence of fused aromatic ring and enhanced planarity. All the metal complexes have potent to bind with receptor than the ligand. The complexes reported in this article have potential as observed from the data and they are proposed for further studies such as anticancer agents.

Acknowledgments

Disclosure statement

No potential conflict of interest was reported by the authors.

References

[1] D.S. Sigman, A. Mazumder, D.M. Perrin, M.Z. Wang, Z.X. Meng, B.L. Liu, G.L. Cai, C.L. Zhang, X.Y. Wang. *Inorg. Chem. Commun.*, **8**, 368 (2005).
[2] S.M. Abdallah, G.G. Mohamed, M.A. Zayed, M.S. Abou El-Ela. *Spectrochim. Acta A Mol. Biomol. Spectrosc.*, **73**, 833 (2009).

[3]   P.G. Devi, S. Pal, R. Banerjee, D. Dasgupta. *J. Inorg. Biochem.*, **101**, 127 (2007).
[4]   A.M. Abu-Dief, I.M.A. Mohamed. *Beni Suef Univ. J. Basic Appl. Sci.*, **4**, 119 (2015).
[5]   K.S. Abou Melha. *J. Enzyme Inhib. Med. Chem.*, **23**, 493 (2008).
[6]   A.A. El-Sherif, M.R. Shehata, M.M. Shoukry, M.H. Barakat. *Spectrochim. Acta A Mol. Biomol. Spectrosc.*, **96**, 889 (2012).
[7]   (a) Z.-Y. Yang, R.-D. Yang, F.-S. Li, K.-B. Yu. *Polyhedron*, **19**, 2599 (2000);(b) J.L. Buss, J. Neuzil, P. Ponka. *Arch. Biochem. Biophys.*, **42**, 1 (2004).
[8]   L.H. Shargiand, M.A. Nasser. *Bull. Chem. Soc. (Jpn.)*, **76**, 137 (2003).
[9]   J.P. Costes, S. Shova, W. Wernsdorfer. *Dalton Trans.*, **14**, 1843 (2008).
[10]   N.A. Venkariya, M.D. Khunt, A.P. Parikh. *Ind. J. Chem.*, **42B**, 421 (2003).
[11]   P. Lu, M.L. Zhu, P. Yang. *J. Inorg. Biochem.*, **95**, 31 (2003).
[12]   M.K. Taylor, J. Reglinski, D. Wallace. *Polyhedron*, **23**, 3201 (2004).
[13]   S. Chandra, L.K. Gupta. *Spectrochim. Acta A Mol. Biomol. Spectrosc.*, **60**, 1563 (2004).
[14]   R. Ramesh, N. Dharmaraj, R. Karvembu, K. Natarajan. *Ind. J. Chem.*, **39A**, 1079 (2000).
[15]   S. Chandra, R. Kumar. *Transit. Met. Chem.*, **29**, 269 (2004).
[16]   F. Akagi, Y. Michihiro, Y. Nakao, K. Matsumoto, T. Sato, W. Mori. *Inorg. Chim. Acta*, **357**, 684 (2004).
[17]   S. Chandra, S.D. Sharma. *Transit. Met. Chem.*, **27**, 732 (2002).
[18]   S. Khan, S.A.A. Nami, K.S. Siddiqi. *Spectrochim. Acta A Mol. Biomol. Spectrosc.*, **68**, 269 (2007).
[19]   N. Raman, J. Dhaveethu Raja, A. Sakthivel. *J. Chem. Sci.*, **119**, 303 (2007).
[20]   N. Dharmaraj, P. Viswanathamurthi, K. Natarajan. *Transit. Met. Chem.*, **26**, 105 (2001).
[21]   C. Hemmert, M. Pitie, M. Renz, H. Gornitzka, S. Soulet, B. Meunier. *J. Biol. Inorg. Chem.*, **6**, 14 (2001).
[22]   M. Navarro, E.J. Cisneros-Fajardo, A. Sierralta, M. Fernández-Mestre, P. Silva, D. Arrieche, E. Marchán. *J. Biol. Inorg. Chem.*, **8**, 401 (2003).
[23]   E. Canpolat, M. Kaya, A. Yazici. *Spectrosc. Lett.*, **38**, 35 (2005).
[24]   R.C. Maurya, P. Patel, S. Rajput. *Synth. React. Inorg. Met.-Org. Chem.*, **33**, 817 (2003).
[25]   A.P. Mishra, S.K. Gavtarm. *J. Ind. Chem. Soc.*, **81**, 324 (2004).
[26]   M.T. Huang, R.C. Smart, C.Q. Wong, A.H. Conney. *Cancer Res.*, **48**, 5941 (1988).
[27]   M.T. Huang, W. Ma, Y.P. Lu, R.L. Chang, C. Fisher, P.S. Manchand, H.L. Newmark, A.H. Conney. *Carcinogenesis*, **16**, 2493 (1995).
[28]   E.M. Jung, J.H. Lim, T.J. Lee, J.-W. Park, K.S. Choi, T.K. Kwon. *Carcinogenesis*, **26**, 1905 (2005).
[29]   M. Wang, L.F. Wang, Y.Z. Li, Q.Z. Li, Z.D. Xu, D.M. Qu. *Transit. Met. Chem.*, **26**, 307 (2001).
[30]   P. Reddy, Y. Lin, H. Chang. *Arcivoc*, **2007**, 113 (2007).
[31]   Y. Heo, Y. Song, B. Kim, Y.A. Heo. *Tetrahedron Lett.*, **47**, 3091 (2006).
[32]   F. Piscitelli, C. Ballatore, A. Smith. *Bioorg. Med. Chem. Lett.*, **20**, 644 (2010).
[33]   D.P. Fairlie, M.W. Whitehouse. *Drug Des. Discov.*, **8**, 83 (1991).
[34]   N. Priyadharshini, S. Iyyam Pillai, S. Subramanian, P. Venkatesh. *Der Pharma Chem.*, **7**, 186 (2015).
[35]   A.A. El-Sherif. *J. Solut. Chem.*, **41**, 1522 (2012).
[36]   F. Gonzalez-Vilchez, R. Vilaplana, M. Gielen, E.R.T. Tiekink (Eds.). *Metal—Based Diagnostic Agents,* Chap. 12, p. 219, Wiley, New York (2005).
[37]   F. Tisato, C. Marzano, M. Porchia, M. Pellei, C. Santini. *Med. Res. Rev.*, **30**, 708 (2010).
[38]   Y. Wang, X. Zhang, Q. Zhang, Z. Yang. *Biometals*, **23**, 265 (2010).
[39]   K. Užarević, M. Rubčić, V. Stilinović, B. Kaitner, M. Cindrić. *J. Mol. Struct.*, **984**, 232 (2010).
[40]   P. Fita, E. Luzina, T. Dziembowska, C. Radzewicz, A. Grabowska. *J. Chem. Phys.*, **125**, 184508 (2006).
[41]   P.R. Reddy, K.S. Rao, B. Satyanarayana. *Tetrahedron Lett.*, **47**, 7311 (2006).
[42]   H. Deng, J.W. Cai, H. Xu, H. Zhang, L.N. Ji. *Dalton Trans.*, **3**, 325 (2003).
[43]   A. Wolfe, G.H. Shimer, T. Meehan. *Biochemistry*, **26**, 6392 (1987).
[44]   S. Satyanarayana, J.C. Dabrowiak, J.B. Chaires. *Biochemistry*, **32**, 2573 (1993).
[45]   S. Vats, L.M. Sharma. *Synth. React. Inorg. Met.-Org. Chem.*, **27**, 1565 (1997).

[46] B.J. Kennedy, G.D. Fallon, B.M.K. Gatehouse, K. Murray. *Inorg. Chem.*, **23**, 580 (1984).
[47] H. Temel, S. Ilhan, M. Sekerci, R. Ziyadanogullari. *Spectrosc. Lett.*, **35**, 35 (2002).
[48] K. Nakamoto. *Infrared and Raman Spectra of Inorganic and Coordination Compounds*, 4th Edn, Wiley, New York (1986).
[49] G.M. Abu El-Reash, O.A. El-Gammal, M.M. El-Gamil. *Spectrochim. Acta A Mol. Biomol. Spectrosc.*, **104**, 383 (2013).
[50] A.B.P. Lever. *Inorganic Electronic Spectroscopy*, 2nd Edn, Elsevier, New York, p. 355 (1984).
[51] B. Niladri, A. Chaudhuri, C. Sibani, R.C. Chirantan. *Inorg. Nano-Met. Chem.*, **48**, 495 (2018).
[52] S. Srinivasan, G. Rajagopal, P.R. Athappan. *Transit. Met. Chem.*, **26**, 588 (2001).
[53] B.J. Hathaway, B. Walsh. *J. Chem. Soc., Dalton Trans.*, **108**, 681 (1980).
[54] B.M. Zeglis, V.C. Pierre, J.K. Barton. *Chem. Commun.*, **44**, 4565 (2007).
[55] F. Arjmand, M. Aziz. *Eur. J. Med. Chem.*, **44**, 834 (2009).
[56] S. Roy, A. Bauza, A. Frontera, F. Schaper, R. Banik, A. Purkayastha, B.M. Reddy, B. Sridhar, M.G.B. Drew, S.K. Das, S. Das. *Inorg. Chim. Acta*, **440**, 38 (2016).
[57] N. Raman, A. Selvan. *J. Coord. Chem.*, **64**, 534 (2011).
[58] X.L. Wang, H. Chao, H. Li, X.L. Hong, L.N. Ji, X.Y. Li. *J. Inorg. Biochem.*, **98**, 423 (2004).
[59] M. Sunita, B. Anupama, B. Ushaiah, C.G. Kumari. *Arab. J. Chem.*, **10**, 3367 (2017).
[60] G. Kumaravel, N. Raman. *Mater. Sci. Eng. C Mater. Biol. Appl.*, **70**, 184 (2017).
[61] P. Jayaseelan, E. Akila, M. Usha Rani, R. Rajavel. *J. Saudi Chem. Soc.*, **20**, 625 (2016).
[62] M.C. Prabahkara, H.S. Bhojya Naik. *Biometals*, **21**, 675 (2008).
[63] G.G. Mohamed. *Spectrochim. Acta A Mol. Biomol. Spectrosc.*, **64**, 188 (2006).
[64] N.A. Negm, M.F. Zaki, M.A.I. Salem. *Colloids Surf. B Biointerfaces*, **77**, 96 (2010).
[65] R. Ramesh, S. Maheswaran. *J. Inorg. Biochem.*, **96**, 457 (2003).
[66] N.O. Gopal, H.H. Lo, S.C. Ke. *J. Am. Chem. Soc.*, **130**, 2760 (2008).
[67] A. Arunadevi, R. Paulpandiyan, N. Raman. *J. Mol. Liq.*, **241**, 801 (2017).
[68] N. Raman, T. Chandrasekar, G. Kumaravel, L. Mitu. *Appl. Organomet. Chem.*, **32**, 3922 (2018).

Google

ISSN number for Inorganic Chemistry Communications   ✕ | 🔍

Q All   📰 News   🖼 Images   ⌾ Shopping   ◉ Maps   ⋮ More   Tools

About 1,43,00,000 results (0.53 seconds)

1387-7003

Additional details

Cited half-life	5.10
Website description	Inorganic Chemistry Communications website
Other titles	Inorganic chemistry communications (Online)
Print ISSN	1387-7003
OCLC	41970220

6 more rows

https://www.researchgate.net › journal › Inorganic-Chemi...
Inorganic Chemistry Communications - ResearchGate

❓ About featured snippets · 🚩 Feedback